M. OTTE (éd.), **Nature et Culture**, Colloque de Liège (13-17 décembre 1993), Liège, E.R.A.U.L. 68, 1995, p. 63 à 78.

PALAEOENVIRONMENTAL INVESTIGATIONS IN THE JAMAL CAVE, MOUNT CARMEL, ISRAEL

M. WEINSTEIN-EVRON and A. TSATSKIN*

INTRODUCTION

Unlike its neighbouring caves, Tabun, el-Wad and Skhul, Jamal is the only one of the famous wadi el-Mughara caves which has never been excavated before. The caves are situated in a reefal limestone on the southern escarpment of the wadi where it debouches onto the Coastal Plain about 20 km south of Haifa (Fig. 1). Jamal cave was tested by Garrod but "was found to be practically empty of deposits; only a skin of breccia, apparently of Mousterian Age, remained in patches on the rock, and a few Early Bronze Age sherds and flints were found in a depression in the floor" (Garrod and Bate, 1937:4). This was later supported by Olami (1984:111) who stated that "shepherds have almost completely cleared the cave, which was not found suitable for excavation remains of breccia found at the entrance and on the posterior wall of the cave, with a few patches on the western wall also". However, recent excavations in the cave (Weinstein-Evron and Tsatskin, n.d.) have revealed that the brecciated archaeological layers cover the entire cave floor and are not restricted to patches as was previously thought.

Jamal Cave consists of one chamber, measuring 12x9 m, with a small niche in its western part (Fig.2). The surface of the cave floor dips strongly from the southeast towards the centre. Garrod's 'depression in the floor' turned out to be an elliptic, karstic pit in the western part of the cave. The sediments seem to be arranged concentrically around this pit, probably as a result of secondary processes related to karstic collapse and erosion.

The area excavated to date includes a trench along the 23 line from the eastern wall towards the central part of the cave (Fig. 2), together with selected squares along the K-J line perpendicular to the former 23 line. Bones were not preserved in the cave and pollen or other botanical material could not be extracted. Thus, our palaeoenvironmental reconstructions are based on geological observations and micromorphological analyses only. These can assist in reconstructing processes of deposition as well as post-depositional changes, including human impact (Courty *et al.*, 1989).

* Zinman Institute of Archaeology, University of Haifa, 31905 Haifa, Israel

GEOLOGICAL OBSERVATIONS

Two distinct groups of sediments have been identified: 1) sediments which lie upon the bedrock and are represented in the section from the southern face of the trench along the 23 line (Fig. 3); 2) sediments from the central part of the cave. A lithological disconformity between these two groups of sediments was observed, testifying to a probable chronological hiatus. The relationships between these two groups of sediments are not fully understood yet, since only the upper part of the sediments belonging to the second group has been excavated to date. It is for this reason that the stratigraphic units of the second group are labelled separately.

Three main stratigraphic units were distinguished within the sediments of the first group. All are inclined towards the centre of the cave and exhibit vertical and lateral disconformities. The geological sequence is described from top to bottom:

- Unit 1 : greyish-yellow, silty clay loam cemented to hard breccia, 0-20 cm thick, with ochre-yellow mottles and thin reddish lenses. There are abundant loose carbonate nodules. Unit 1 contains scarce lithics of Middle Palaeolithic age, including a side scraper (Fig. 4: 4) and two Levallois flakes (Fig. 4:6-7).

- Unit 2 : reddish clay loam also cemented to hard breccia, up to 40cm thick, with ochre-yellow and cinnamon dots and abundant carbonate nodules. Subunit 2a adheres to the bedrock wall and differs from main Unit 2 by its redder hue and texture; Subunit 2b is an intercalation of ochre-yellow soft material. Lower Palaeolithic artifacts were found in Unit 2, including bifaces (Fig. 5:1,2) and scrapers (Fig. 5:3; Fig. 4:2-3) and others (Fig. 4:1). The small bifaces and relatively thick scrapers in Unit 2 suggest a probable Acheuleo-Yabrudian (Mugharian) affinity, similar to Tabun E.

- Unit 3 : is softer, less cemented and browner clay loam, with small lenses of greyish material. The lithic finds in Unit 3 are too scarce to enable cultural designation.

The second group of sediments has been tentatively divided into four subunits (Fig. 2), based on field observations and microfabric analyses. Unit a : greyish-yellow loam, with black convoluted exfoliated intercalations. Unit b : compacted yellow-brown silty clay. Unit c : greenish loam with spots of white carbonate concretions. Unit d : hard greyish breccia marking the outer rim of the 'pit'. Sediments of the second group contain scarce Middle Palaeolithic items (Fig. 4 : 8-9).

The main lithic element in all the layers are waste products (Weinstein-Evron and Tsatskin, n.d.), followed by flakes, tools (many of which are partially retouched flakes) and cores (e.g. Fig. 4:5, from Unit 2). Various analyses, such as refitting, were not feasible on this small sample. Still, the general composition of the assemblages suggests some kind of workshop activity.

MICROMORPHOLOGY

Micromorphological analysis, coupled with scanning electron microscope (SEM) and microprobe analyser (EXDRA) were employed. The results of the analysis of characteristic samples from each group of sediments are given. The description of petrographic thin sections primarily follows the terminology of Bullock et al. (1985).

Microfabric of sediments of the first group is shown in Fig. 6 (for location of samples, see Fig. 3):

Sample L23-6 (Unit 3) (Fig. 6: a,b). It is an heterogeneous, microaggregated carbonate-free clay loam with *ca.* 10% fine sand of subangular quartz and some 30-40% silt. The sediment is composed of yellow and dark reddish-brown rounded aggregates, ranging from 0.05 mm to 2.5 mm in thickness. Various phosphatic pseudomorphs embedded among them apparently originated from *in situ* diagenetic alteration of bones. Light-coloured aggregates (probably because of Fe reduction) show strong birefringence of granostriated and reticulated types. In contrast, dark-coloured aggregates are almost isotropic, owing to fine comminution of charred organic matter (OM). Channel porosity is well developed. All the vughs and channels are infilled with multilaminated phosphatic coatings or with compound fibrous infillings.

Sample L23-5 (Unit 2) (Fig.6:c). This sediment is even more heterogeneous than the former one. Sparitic calcite infillings occupy up to 30% of the thin section area. Red decalcified (rubefied) aggregates, ranging from 0.5 to 2.0 mm, are composed of well sorted silty clay associated with Fe-humic compounds or finely disseminated charred organic particles. Granular sparitic incrustations, completely infilling pores, seem to be responsible for the over-compaction of the sediment. A few localities clearly indicate that phosphatic precipitations are superimposed by calcite impregnations.

Sample L23-5a (Subunit 2b) (Fig 6:d). In contrast to unit 2, no sparitic infillings in pores were observed. Only two corroded microsparitic nodules were found in one of the channels. This unit is characterized by various phosphatic pseudomorphs in the groundmass. Local concentrations of pellets indicate high-intensity biological activity.

Sample L23-2 (Unit 1) The sediment is characterized by increased amounts of dark-coloured (coprogenic?) isotropic soil microaggregates, embedded in a compacted birefringent ooid groundmass. Microaggregates are disrupted locally and planar voids are infilled with limpid apatite infillings.

The patchy, residual occurrence of the lowermost layer (Unit 3), immediately over the bedrock, testifies to heavy erosion following the deposition of this layer. Micromorphological heterogeneity could have been enhanced during this episode of geomorphic instability. Poor sorting of sand grains in the clay loam points to the complex mode of deposition and redeposition of the sediment. Decalcification and localized discolouration of particular microaggregates can be accounted for by humid conditions inside the cave, favouring gleying effects. Biological activity is inferred from the incorporation of organic particles, possibly of anthropogenic origin, into the strongly phosphatized groundmass.

Increased aeolian input characterizes the silty clay loam of Unit 2. It seems plausible that charred organic particles and 'rubefied' microaggregates were incorporated into the sediment at the time of human occupation, under relatively humid conditions favouring soil ripening. Later, the rubefied aggregates were disrupted in the course of repeated wetting and drying. The intraaggregate cracks were subsequently infilled with secondarily precipitated phosphates. The abundant sparitic calcite impregnations within the sediments are most probably related to a much later diagenetic episode, during and/or following inundation of the cave. The excess of water would have caused or intensified both karstic slumping and partial erosion of sediments, resulting in the observed lateral disconformities.

The microfabric of the upper Unit 1 is characterized by high coprogenic aggregation and by features of anthropogenic input of organic materials. These were subsequently secondarily reworked in the course of geomorphic activation. Severe diagenetic transformations are clearly attested to by an overall calcite cementation and by ductile deformations of Mn-rich laminae in some spots.

Three selected samples from the second group of sediments are discussed (Fig. 7):

Sample K23-4 (Unit a) (Fig. 7: a, b). Microaggregation reaches its maximum throughout this unit, showing many compound polyphase ooids. The groundmass is completely decalcified and contains opaque black flakes in the groundmass; the same material forms a thin black coating on the fissure walls. X-ray studies revealed the presence of manganese oxides in the form of cryptomelan in this layer. However, in thin sections the coatings are anisotropic, red-hued and may be also associated with other substances, e.g., clay, phosphorous, iron and organic matter. The input of manganese-bearing solutions could have occurred at the time of karstic collapse and inundation in the cave. The impact of human activity (e.g. hearths) on the composition of the black intercalations should not be ruled out.

In order to clarify the nature of the complex microfabric in this unit, we have employed SEM equipped with a microprobe. These submicroscopic analyses emphasize the complex internal fabric of the black-coloured coatings and concentrations in the groundmass. As a rule, they consist of silt-sized nodules (about 0.005 mm), enveloped with very thin phosphatic coatings. The nodules themselves are composed of clay minerals intermixed with manganese and phosphatic minerals (Fig. 8).

Sample J21-1 (Unit b) (Fig. 7: c,d). Three main components can be distinguished in this heterogeneous sediment: well-shaped vughy patches of strongly phosphatized material; clay with comminuted charred organic matter; and fluidal stripes of brown-stained micritic calcite which incorporate small soil aggregates and charcoal shreds of ca. 0.05 mm in length.

Sample J21-4 (Unit c) (Fig. 7: e,f). This sediment is more silty and better sorted. The ooid microstructure was not be observed and the silty clay groundmass is isotropic, probably as a result of intimate comminution of charred organic matter. Secondarily precipitated phosphates are presented, either by homogeneous phosphatic infillings in large channels and vughs, or by brown crystallizations associated with calcite micritic impregnations within voids. In the latter case, phosphatic precipitation post-dates calcite accumulation.

The calcified silty sediments of the second group (the central part of the cave) reflect the strong impact of phosphorus-bearing (guano-derived?) solutions over the mineral mass. This is evidenced by abundant limpid phosphatic coatings within the pore space. Furthermore, micritic calcite neoformations show signs of phosphatic impact.

DISCUSSION AND CONCLUSIONS.

Palaeoenvironmental reconstructions largely depend on our ability to differentiate between depositional and post-depositional processes.

Processes of sedimentation. The sediments in Jamal Cave are hard, strongly brecciated and contain high amounts of clay. It is difficult to source the fine material with confidence, as clay could have been either wind-blown or derived from colluvial input of clayey soil material through run-off. Moreover, the possibility of *in situ* weathering of the parent rock in the cave should not be ruled out. Such a weathering could have occurred during the phreatic stage of the cave development, long before human habitation in the cave. Most probably, the Jamal Cave sediments have accumulated from different sources, exhibiting a complex way of sedimentation. Their tracing is difficult, however, because the sediments have been drastically altered by later diagenetic processes.

Processes of diagenesis and weathering. Post-depositional modifications of Jamal Cave sediments are related both to karstic and erosional processes and to biological and chemical transformations of pristine materials.

Colluviation and karstic slumping. Active erosional processes are well documented by numerous notches and scours upon the surface of the sedimentary fill, as well as by the patchy appearance of the geological units and disconformities between them. One of the best examples for these disconformities is represented by the distortion of the black-coloured, manganese-enriched laminae in Unit a. The secondary redeposition of the sediments is also confirmed by micromorphological features, such as the heterogeneous microfabric of all the units, and, in particular, the ooid type of microaggregation. Interestingly, ooids characterize mainly the first sedimentary group, while the second is largely devoid of this type of microaggregation, suggesting only minor lateral movement. The ooid microstructure of Unit a can be related to the transitional position of this Unit, which is between the two groups of sediments.

Ooids could have originated in dynamic geomorphological situation, probably under conditions of water saturation (Mücher and Morozova, 1983). Their formation may imply an episode of an inundation of the cave which could have evoked karstic activity and colluviation. Our field observations and micromorphological data indicate that several phases of collapse could have occurred throughout the geological history of the cave, with the major collapse probably taking place during and/or after the accumulation of unit 2. It is not yet clear whether atmospheric water or ground water caused this flooding in Jamal. However, this inundation undoubtedly exerted a significant impact on the sediments and on the poor state of preservation of, for example, anthropogenic remains.

Biological, anthropogenic and geochemical transformations. Because of the mechanical disturbances and the supposed inundation, these are sometimes hard to identify. Still, various calcite, phosphatic and manganese neoformations are good indicators of the high degree of weathering, as well as of harsh geochemical changes in the cave. The geochemical alteration of minerals and organic materials would have been particularly intensive during periods of inundation. As mentioned earlier, bones are not preserved in the cave. Phosphate minerals, which are the most common in the cave, are well recognized in two basic micromorphological forms: in pellets, suggesting *in situ* formation from chips of bones, and in void coatings indicating precipitation from mobile solutions. Strong phosphatization has also been reported from other Mount Carmel caves, particularly from Tabun (Goldberg,1973; Jelinek *et al.*, 1973; Goldberg and Nathan, 1975) and Kebara (Goldberg and Laville, 1991). Anthropogenic features and organic material are hardly discernible in the Jamal sequence. Though no indications for hearths were recognized in the field, the micromorphology indicates almost everywhere the presence of comminuted charred organic materials, probably derived from ashes. Furthermore, it is tempting to suggest that the manganese oxides, found in Unit a, were formed by oxidation-reduction processes of carbon-bearing materials under gleying conditions. Pellets and bioaggregates also testify to processes of biological activity.

INTENSITY OF DIAGENETIC TRANSFORMATION

Recent studies in south Levantine caves also indicate complex modes of deposition and intensive post-depositional processes (e.g., Goldberg, 1973; Goldberg and Laville, 1991). However, as compared to the evidence from Jamal Cave, it seems that in none of these caves did diagenetic processes reach the degree observed in Jamal. The substantial diagenesis in Jamal could have been the result of longer and/or more intensive secondary processes than in the other caves. In the neighbouring Tabun Cave, sediments of roughly the same age exhibit a much better state of preservation. Thus, it seems that the Jamal sediments underwent a stronger diagenetic alteration. This can be attributed, at least partially, to the small size of the cave which renders it most susceptible to erosional processes, especially those related to ground water fluctuations. It is most probable that this post-depositional diagenesis accounts for the total disappearance of bones and other organic material from the sediments. In these periods of inundation, the cave was unfit for human occupation.

In summary, the Jamal Cave contains lithic industries, found in a very complex sedimentary setting, with numerous signs of erosion and diagenesis. In spite of the small samples, two distinct cultural assemblages can be defined: Lower Palaeolithic (probably Acheuleo-Yabrudian) and Middle Palaeolithic. It is thus roughly contemporaneous to the detailed sequence in the neighbouring cave of Tabun (Garrod and Bate, 1937). In view of the intense secondary reworking of the sediments in Jamal, the possibility of a Lower Palaeolithic assemblage, in which Middle Palaeolithic artifacts were incorporated in the course of long and intense post-depositional erosional processes, should not be ruled out. In fact it seems posibble that the Jamal sediments studied to date have been largely redeposited by colluviation and karstic slumping from the original, richer archaeological layers. Such layers probably still exist along the walls of the cave. This may also account for the paucity of lithics.

It is further suggested that any discussion of the function of the site should take into account the proximity to Tabun. The two caves most probably belonged to a single socioeconomic system in which the smaller Jamal Cave, served as an 'annexe' to Tabun and must have played a relatively minor role at any given time.

ACKNOWLEDGEMENTS

In spite of the fact that Tabun and Jamal were probably parts of the same cultural complex and existed within a single hydrogeological system, direct correlations between the two caves are problematic. This is due not only to the small lithic assemblages from Jamal, but especcialy to the fact that no distinct levels were identified there. Thus, the Jamal sequence may correlate to only specific portions of the long Tabun sequence or it may represent a 'compacted' Tabun sequence.

We wish to thank Dr. D. Kaufman for his comments and assistance in editing the manuscript. The Jamal excavations are supported by the Israeli Natural Reserves Authority, the Zinman Institute of Archaeology, Irene Levi-Sala CARE Archaeological Foundation, and Schussheim Foundation. The generous funding of the Wolfson Family charitable Trust is gratefully acknoledged. We are indebted to Dr. S. Ilani for field discussions and X-ray analysis, and to Irit Zohar for computer graphics assistance. Special thanks are due to Dr. I. Hershkovitz for his invaluable and enthusiastic support throughout.

REFERENCES

BULLOCK P., FEDOROFF N., JONGERIUS A., STOOPS G. and TURSINA T., 1985,
Handbook for Soil Thin Section Description. Wolverhampton, Waine Research Publications.

COURTY M.A., GOLDBERG P. and MACPHAIL R., 1989,
Soils and Micromorphology in Archaeology. Cambridge University Press.

GARROD D.A.E. and BATE D.M.A., 1937,
The Stone Age of Mount Carmel. Vol 1, Oxford, Clarendon Press.

GOLDBERG P., 1973,
Sedimentology, Stratigraphy and Paleoclimatology of Et-Tabun Cave, Mt. Carmel, Israel. Unpublished Ph.D. Thesis, University of Michigan.

GOLDBERG P. and LAVILLE H., 1991,
Étude geologique des depots de la grotte de Kebara (Mont-Carmel): Campagnes 1982-1984. In: Bar-Yosef, O. and Vandermeersch, B. (eds.), *Le squelette Mousterien de Kebara* 2, Paris, CNRS: 29-41.

GOLDBERG P. and NATHAN Y., 1975,
The phosphate mineralogy of et-Tabun Cave, Mount Carmel, Israel. *Mineralogical Magazine*, 40, 253- 258.

JELINEK A.J., FARRAND W.R., HAAS G., HOROWITZ A. and GOLDBERG P., 1973,
New excavations at the Tabun Cave, Mount Carmel, Israel. *Paleorient* 1: 151-183.

MÜCHER H.J. and MOROZOVA T.D., 1983,
The application of soil micromorphology in Quaternary geology and geomorphology. In: Bullock, P. (ed.). *Soil Micromorphology, 1. Techniques and Applications*, Berkhamsted, A B Acad. Publ.:151-194.

OLAMI Y., 1984,
Prehistoric Carmel. Israel Exploration Society, Israel.

WEINSTEIN-EVRON M. and TSATSKIN A., n.d.,
The Jamal Cave is not empty : Recent discoveries in the Mount Carmel Caves, Israel. *Paleorient* 20/2 (in press).

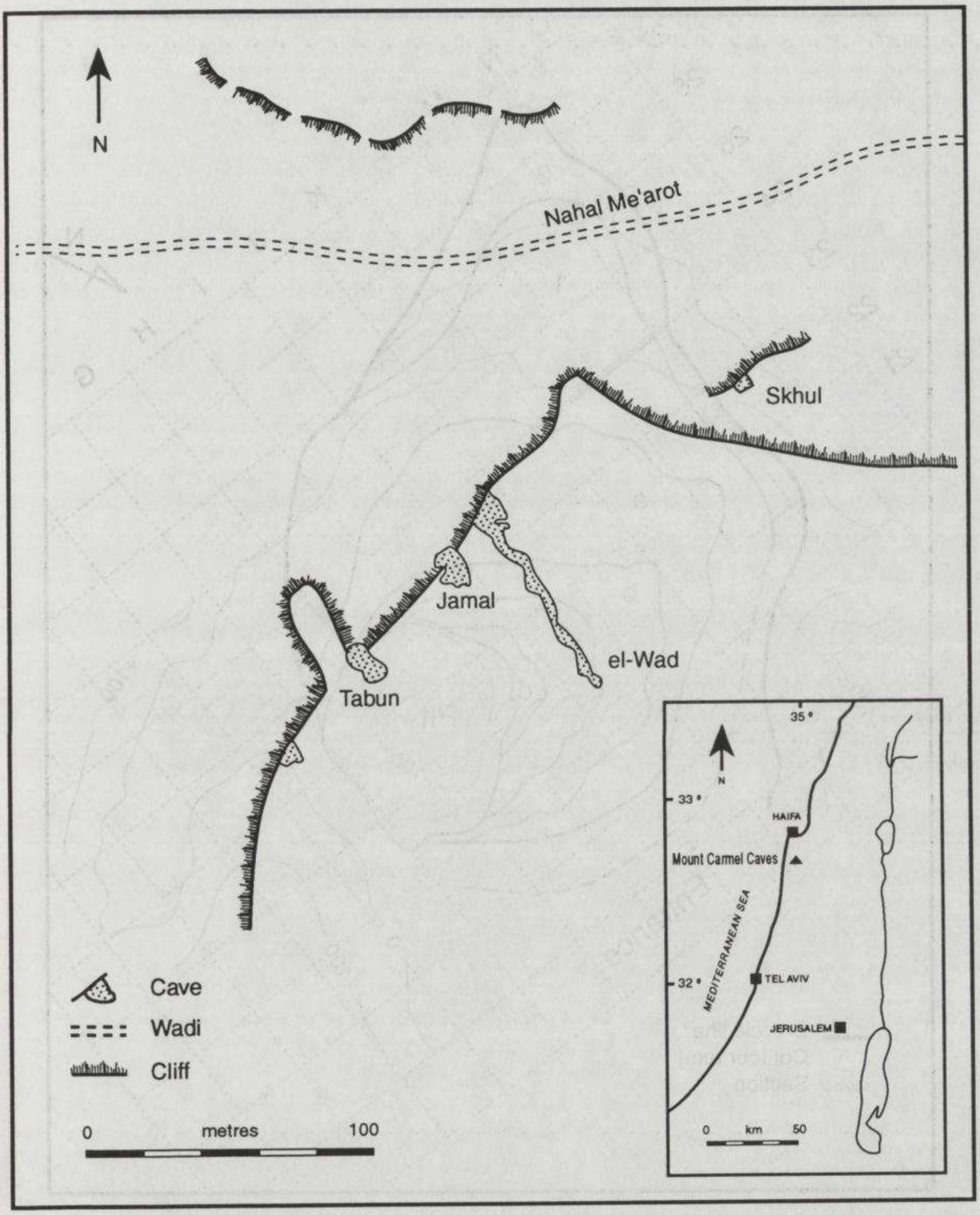

Fig. 1 : Location map.

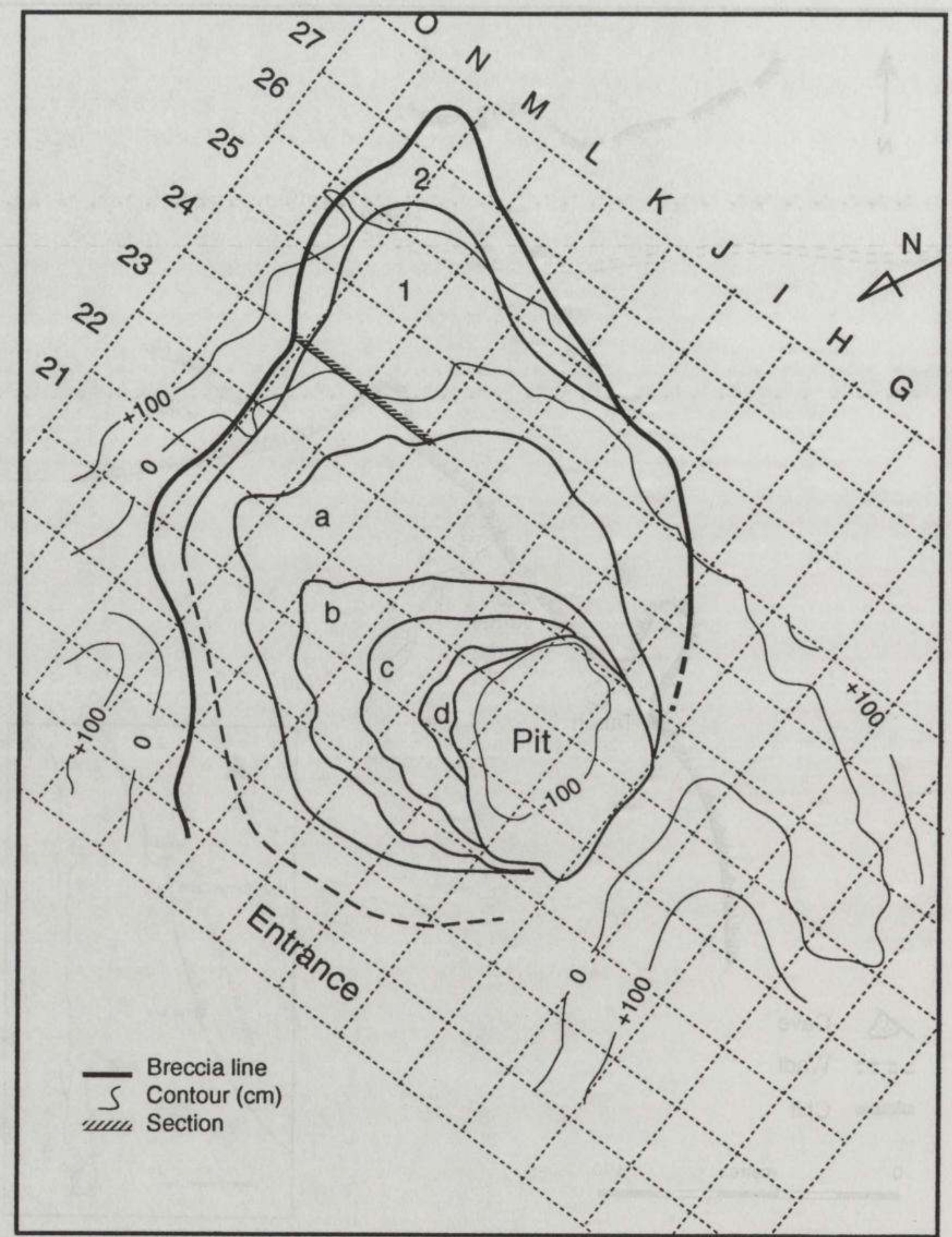

Fig. 2 : Ground plan of the cave showing the concentric arrangement of the main stratigraphic units. 1 - silty clay loam; 2 - phosphatised clay loam; 3 - reddish clay loam; 4 - CaCO3 concretions; 5 - phosphatic mottles; 6 - gleying features; 7 - bedrock; 8 - samples.

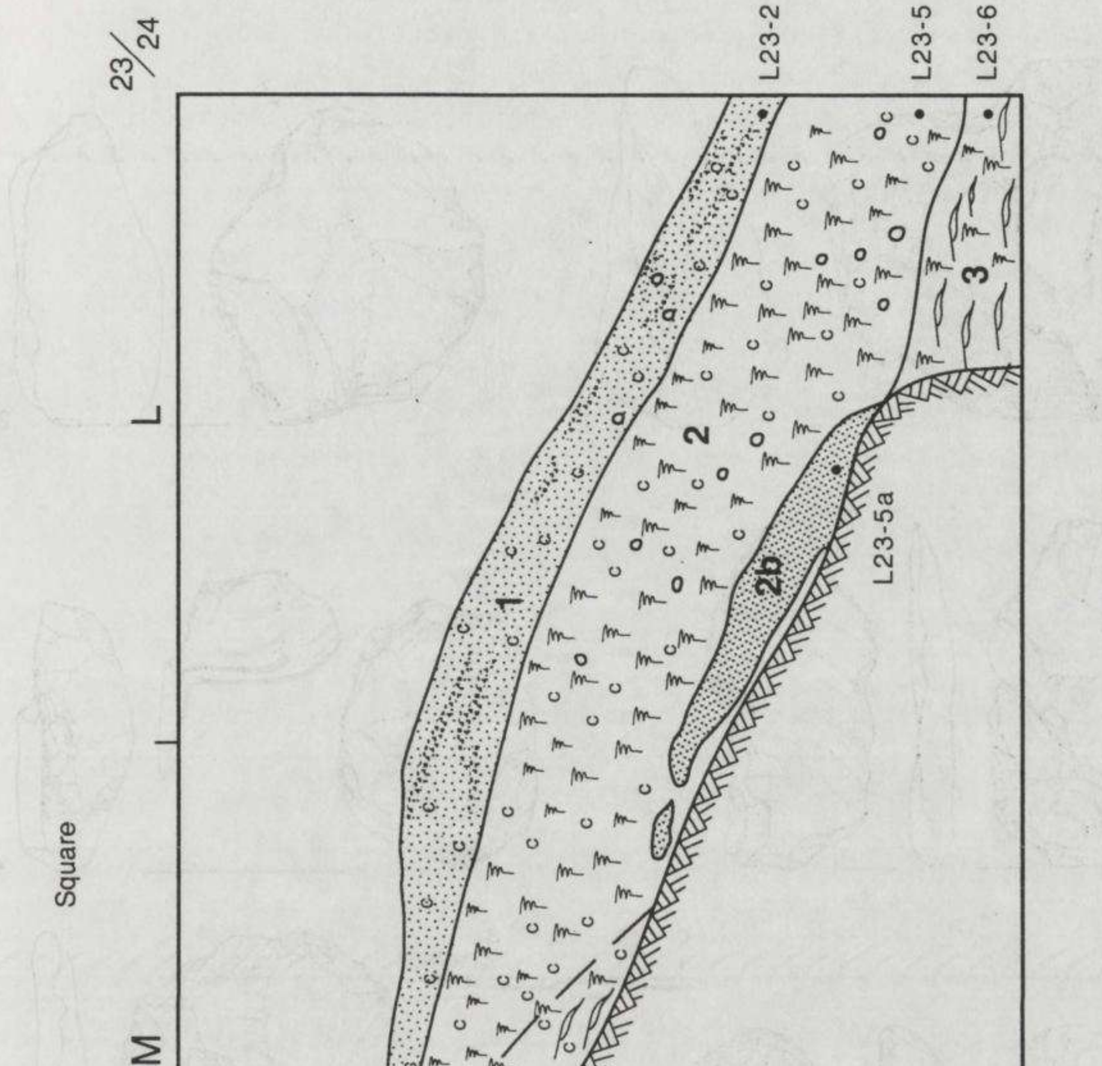

Fig. 3 : The southern wall of the east-west section along the 23 line. For location of the section, see Fig. 2.

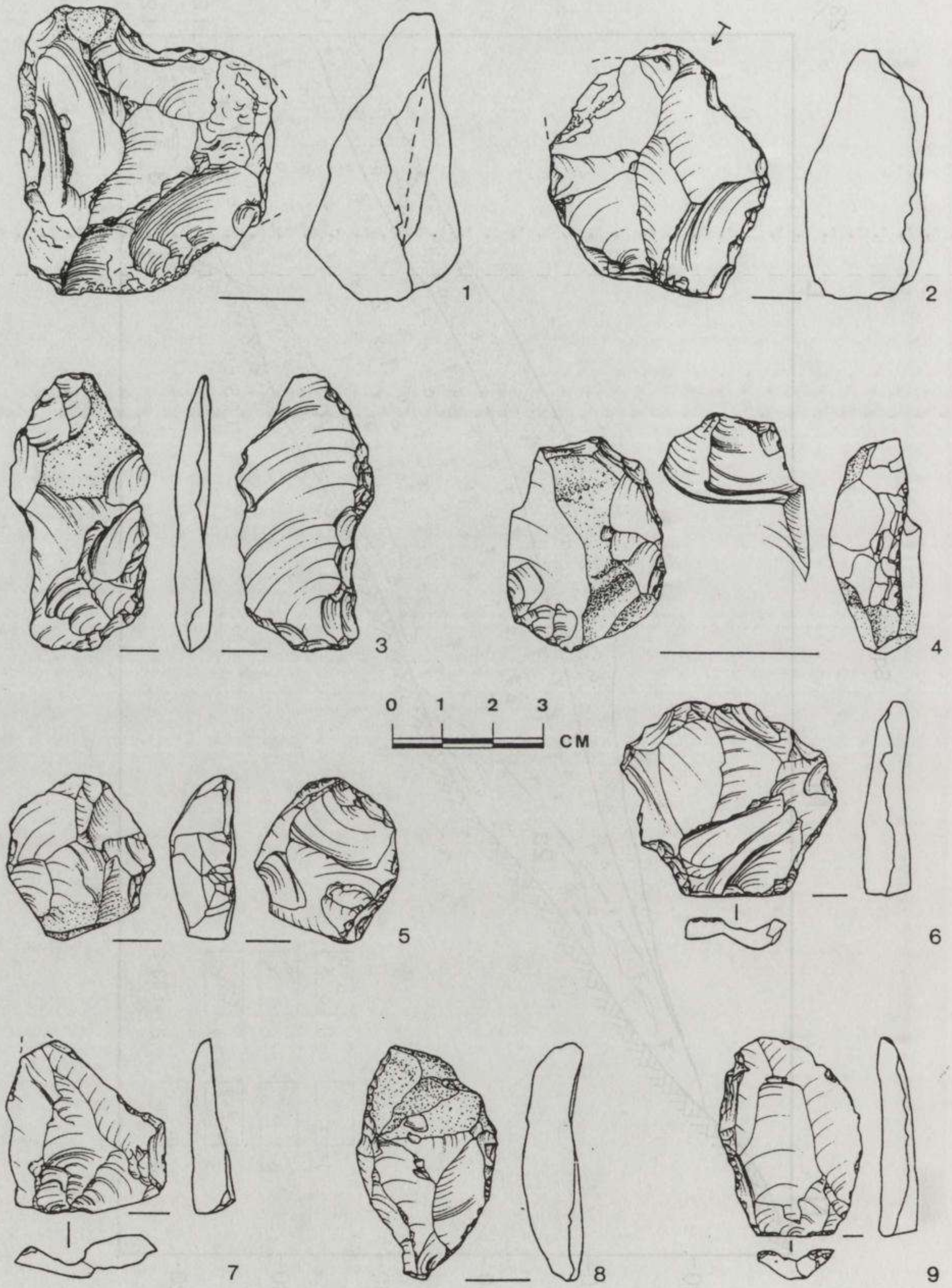

Fig. 4 : Finds from Unit 2 (1-3, 5), Unit 1 (4, 6-7) and Unit a (8-9). 1- notch; 2-4, 8-9 side scrapers; 5- core; 6-7 Levallois flakes (from Weinstein-Evron and Tsatskin, n.d.).

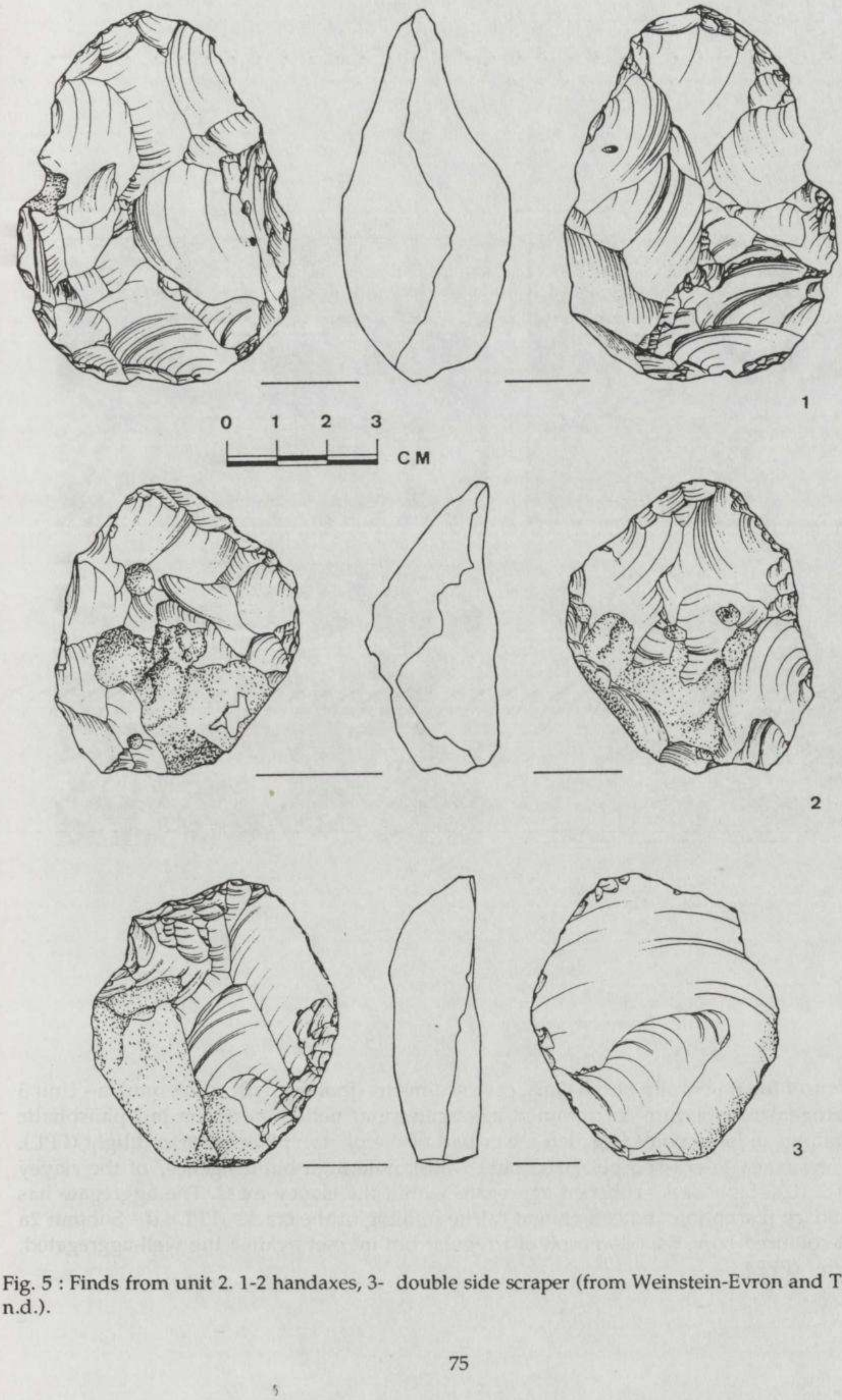

Fig. 5 : Finds from unit 2. 1-2 handaxes, 3- double side scraper (from Weinstein-Evron and Tsatskin, n.d.).

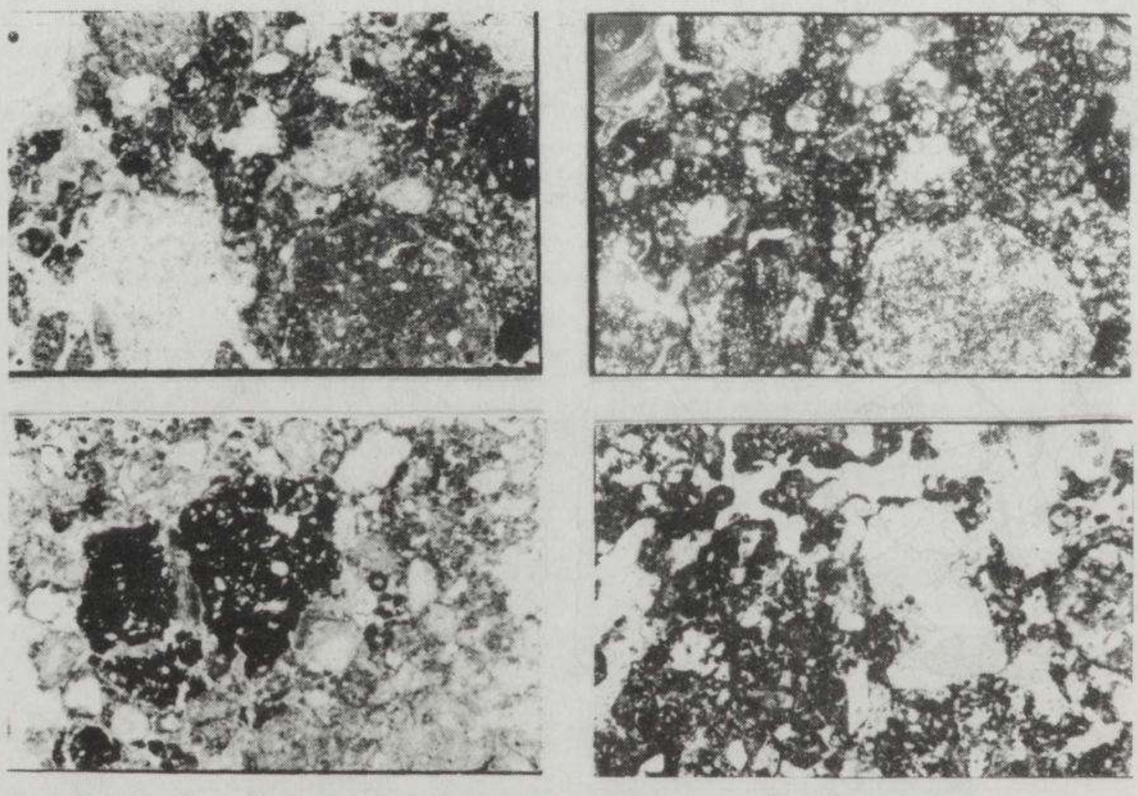

Fig. 6 : Microfabric of the first group of the Jamal cave sediments (frame length is 2.8 mm). a - Unit 3 (L23-6), an heterogeneous mixture of rounded aggregates and pellets with limpid phosphatic coatings and infillings in large pores (e.g., left lower part of the photo); plane polarized light (PPL). b - the same view taken in crossed polarized light (XPL); note high birefringence of the clayey matrix. c - Unit 2 (L23-5), a dark rubefied aggregate within the clayey mass. The aggregate has undergone secondary disruption and consequent calcite infilling of the cracks (PPL). d - Subunit 2a (L23-5a), a light-coloured bone pseudomorph of irregular outline, set against the well-aggregated, decalcified matrix (PPL).

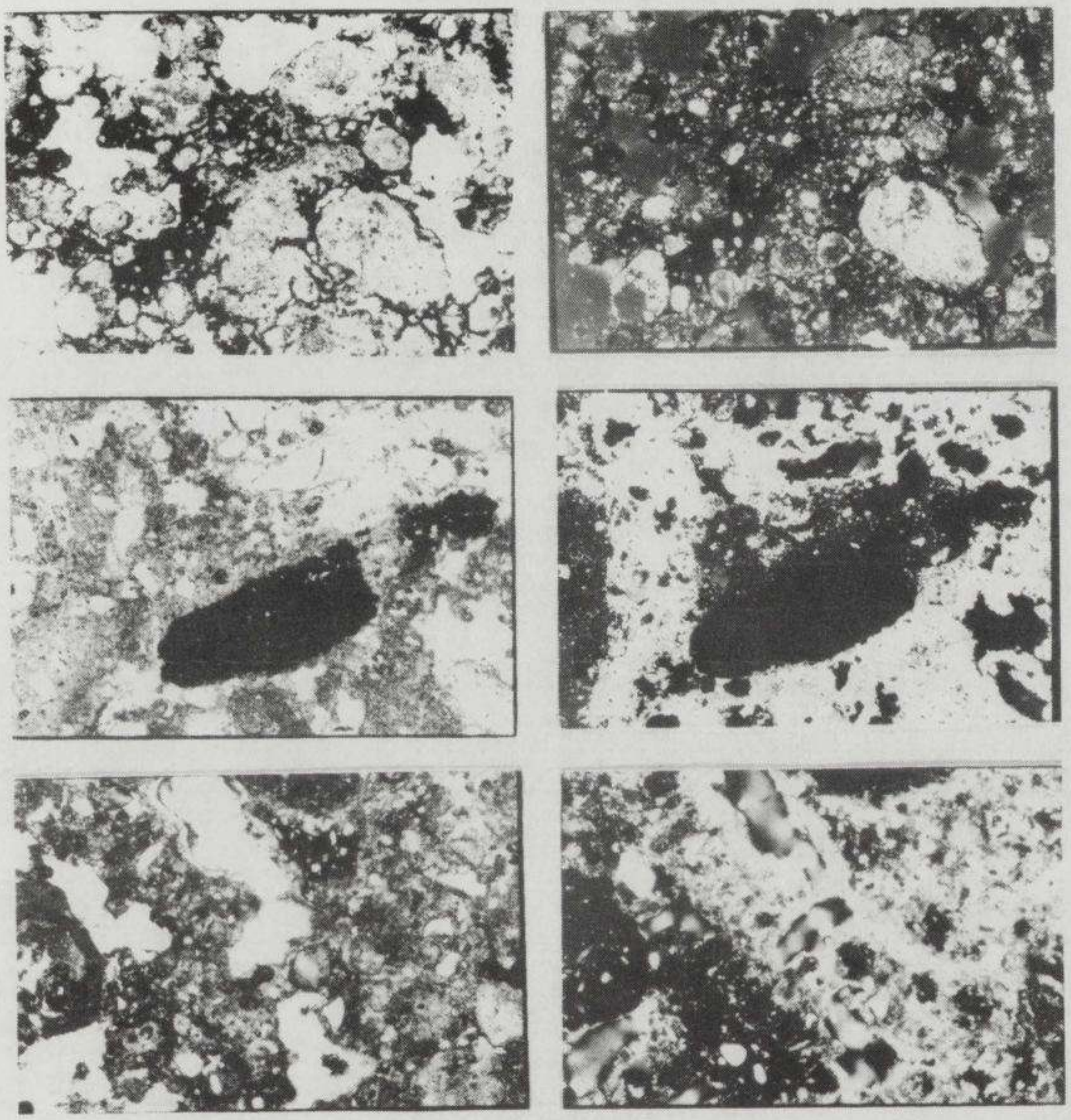

Fig. 7 : Microfabric of the second group of the Jamal cave sediments (frame length is 2.8 mm). a - Unit a (K23-4), a complex ooid microstructure with abundant black manganese coatings (PPL). b - the same view in XPL, showing high birefringence of decalcified matrix, especially in larger ooids. c - Unit b (J21-1), a charred, elongated organic matter embedded in dense disaggregated groundmass (PPL). d - the same view in XPL, showing locally high impregnation of micritic calcite. e - Unit c (J21-4), figurate pores within the matrix which contains comminuted organic materials (PPL). f - the same view in XPL; note the homogeneous phosphatic infillings superimposed upon the thin calcite coatings on the walls of the pores.

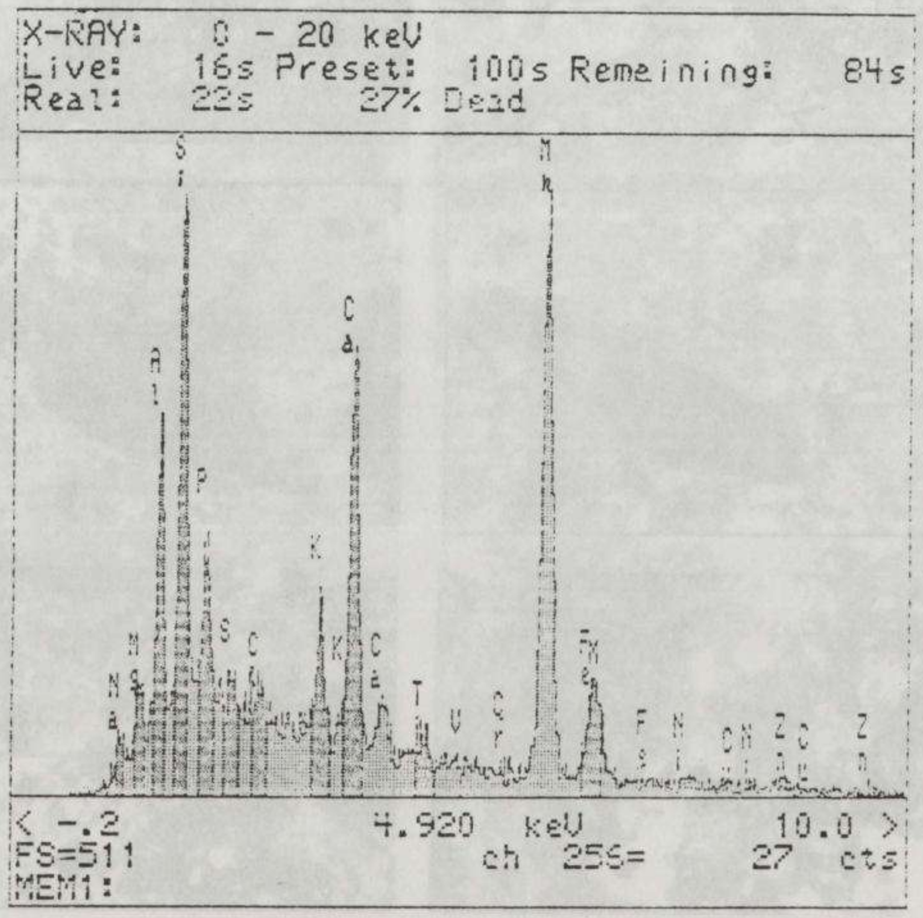

Fig. 8 : Elemental composition of a manganese nodule in Unit a. Note peaks of Si, Ca and Mn.